Quantum dynamics study on the CHIPR potential energy surface for the hydroperoxyl radical: The reactions O + OH⇋O2 + H

Article *in* The Journal of Chemical Physics · January 2015

DOI: 10.1063/1.4905292 · Source: PubMed

2 authors, including:

Antonio J. C. Varandas
University of Coimbra
429 PUBLICATIONS **9,195** CITATIONS

SEE PROFILE

Quantum dynamics study on the CHIPR potential energy surface for the hydroperoxyl radical: The reactions O + OHO2 + H

Marc Moix Teixidor and António J. C. Varandas

Citation: The Journal of Chemical Physics **142**, 014309 (2015); doi: 10.1063/1.4905292
View online: http://dx.doi.org/10.1063/1.4905292
View Table of Contents: http://scitation.aip.org/content/aip/journal/jcp/142/1?ver=pdfcov
Published by the AIP Publishing

Quantum dynamics study on the CHIPR potential energy surface for the hydroperoxyl radical: The reactions O + OH ⇋ O_2 + H

Marc Moix Teixidor and António J. C. Varandas[a)]
Departamento de Química and Centro de Química, Universidade de Coimbra, 3004-535 Coimbra, Portugal

(Received 24 October 2014; accepted 19 December 2014; published online 6 January 2015)

Quantum scattering calculations of the $O(^3P) + OH(^2\Pi) \rightleftharpoons O_2(^3\Sigma_g^-) + H(^2S)$ reactions are presented using the combined-hyperbolic-inverse-power-representation potential energy surface [A. J. C. Varandas, J. Chem. Phys. **138**, 134117 (2013)], which employs a realistic, *ab initio*-based, description of both the valence and long-range interactions. The calculations have been performed with the ABC time-independent quantum reactive scattering computer program based on hyperspherical coordinates. The reactivity of both arrangements has been investigated, with particular attention paid to the effects of vibrational excitation. By using the *J*-shifting approximation, rate constants are also reported for both the title reactions. © *2015 AIP Publishing LLC*. [http://dx.doi.org/10.1063/1.4905292]

I. INTRODUCTION

The detailed understanding of a gas phase reaction is a challenging problem. Despite the enormous progress on the employed methodologies, both experimental and theoretical, the amount of information involved and intricacy of the reactive problem are enormous even in the case of reactions with only a few atoms. In the present work, we study the reactions $O(^3P) + OH(^2\Pi) \rightleftharpoons O_2(^3\Sigma_g^-) + H(^2S)$ with a time-independent methodology to determine their rate constants (thermal rate coefficients) at low temperatures. In particular, the forward reaction is one of the most studied because of its intrinsic importance, e.g., on O_2 production at ultra-low temperatures,[1] and removal of stratospheric "odd-oxygen" and high-vibrationally excited mesospheric OH.[2] Indeed, detailed information on this reaction is also of great interest in astrophysics, since it has recently been demonstrated that the abundance of molecular oxygen could be explained by taking into account gas-grain interactions,[3,4] which has been underestimated by other astrochemical models[5–10] in relation to experimental measurements of its abundance.[11–16]

Theoretically, the title system is important also as a prototype that accommodates a stable intermediate, with studies in both directions of reaction being rather challenging. For $O + OH \rightarrow O_2 + H$, the reaction is exothermic by ~ 0.7 eV (including the zero-point energy correction) which, jointly with the well depth of the intermediate HO_2 species (~2.4 eV relative to the $H + O_2$ asymptote), hinders the accurate calculation of observables due to the large number of involved quantum states.

When reviewing the literature, specifically for the reaction $O + OH \rightarrow O_2 + H$, there are significant discrepancies that emerge between the available measurements and computed values, with the most recent estimate based on experimental rate constants at low temperature being due to Carty *et al.*[6] who predict a value of $(3.5 \pm 1.0) \times 10^{-11}$ cm^3 molecule^{-1} s^{-1} with little temperature dependence between 39 and 142 K. This underestimates by a factor smaller than two previous experimental data[17–23] and theoretical results. Additional experimental kinetic information for this system can be found in KIDA[24] and UMIST[25] databases, as well as other places[26,27] where IUPAC and NASA recommended data can be found. For the reverse reaction, $H + O_2 \rightarrow OH + O$, experimental and theoretical results are generally in better agreement since the rates are mainly dictated by the reaction endothermicity.[28–36]

The adiabatic potential energy surface (PES) for the reactions $O(^3P) + OH(^2\Pi) \rightleftharpoons O_2(^3\Sigma_g^-) + H(^2S)$ has been studied with different levels of intricacy, with the first global forms extensively employed in dynamical simulations being due to Melius and Blint[37] (MB) and Pastrana *et al.*[38] (so-called double many-body expansion or DMBE IV) PESs. Other available forms are the diatomics-in-molecules of Kendrick and Pack[39] (DIMKP), Troe and Ushakov[40] (TU) and, more recently, the XXZLG PES of Xu *et al.*[41,42] In this work, we will employ the so-called Combined-Hyperbolic-Inverse-Power-Representation (CHIPR)[43,44] form, which is based on the *ab initio* data utilized for the XXZLG PES[41] but employs the CHIPR method of Varandas.[44,45]

The refined XXZLG PES referred above has been addressed to improve the description of long range forces of the system which are known to play an important role at low-temperature regimes (see, for example, the recent review,[46] although simple demonstrations have long been advanced[47,48]). When comparing with the CHIPR PES, the main topographical features are in good agreement, although subtle differences arise at regions of the van der Waals wells both in the reactive and product channels where the long-range behavior should be most influential. A complete description of the CHIPR PES and a comparison with other surfaces is available elsewhere.[43–45]

A major goal of the present work is to study the reaction $O + OH \rightleftharpoons O_2 + H$ on the newly reported CHIPR PES. The focus will be on the thermal rate coefficients of the O + OH reaction at low temperatures and the effect of the long range interactions on the associated dynamics. The work is organized as follows. After some brief historical remarks on Sec. II A,

a)Electronic mail: varandas@uc.pt

the time-independent (TI) method and the J-shifting technique are presented on Sec. II B, being followed by some numerical convergence tests on Sec. II C. The results from the dynamics studies for both reactive channels are reported in Sec. III. Some concluding remarks are in Sec. IV.

II. GENERAL

A. Historical survey: A synopsis

Among the papers in the literature, there are many dynamics studies using PESs with different degrees of sophistication. Calculations have been reported for the OH + O reaction with the quasiclassical trajectory[49–54] (QCT) method, the adiabatic-capture-centrifugal-sudden approximation (ACCSA),[55] and a variety of other approaches that used the DMBE IV PES such as calculations of thermal rate coefficients for the $H + O_2$ reaction by extrapolation of $J = 0$ quantum results[56,57] and using quantum flux auto-correlation functions[58,59] (in this case for both the forward and reverse title reactions); see also references therein.

More related to the present work, thermal rate coefficients at lower temperatures have been calculated by Xu *et al.*[60] using the J-shifting approximation and TI methods, as well as employing body-frame hyperspherical (democratic) coordinates[61] and the improved XXZLG PES. Presented subsequently were differential and integral cross sections,[53,62,63] also employing TI methodologies. In turn, Lique *et al.*[64] reported calculations with the ABC code that account for all values of the total angular momentum (but with restrictions on the coupling of its projection) over a grid of energies ranging from 2.4×10^{-4} to 0.038 eV. Above this energy, the J-shifting approximation has been applied to calculate rate constants and cross sections. The resulting thermal rate coefficients turn out to be at least about 20%-30% larger than the previously published values.

Alongside such a work, Quéméner *et al.*[65] studied the O + OH reaction by quantum dynamics. These authors have reported reaction probabilities and rate coefficients obtained with the TI hyperspherical approach of Pack and Parker[66] on the improved XXZLG[42] and DIMKP[39] forms. Specifically, they calculated[67] elastic, inelastic, and reactive cross sections and rate constants with a newer version of the DIMKP PES. Subsequently, Juanes-Marcos *et al.*[68] reported results for the O + OH($v = 1, j = 0$) reaction and Pradhan *et al.*[69] for O + OH($v = 2,3, j = 0$).

In addition to the above work, further quantum dynamics studies have been carried on the O + OH reactive channel, such as time-dependent wave packet (TDWP) calculations by Ma *et al.*,[70] where state-to-state calculations are reported for the O + OH reaction on the XXZLG PES,[41,42] yielding reaction probabilities at different values of J and differential cross sections. Work by Kłos *et al.*[71] has also appeared, where the vibrational relaxation of the OH($v = 1$) + O system is studied by using the coupled-states statistical capture model on two different electronic states.

Regarding the reverse reaction $H + O_2 \rightarrow OH + H$, several dynamics studies have been performed, starting with quasiclassical trajectory and quasiclassical quantum mechanical threshold (QCT-QMT) calculations of thermal rate coefficients by Miller[72] on the MB PES.[37] Similarly, quasiclassical trajectory studies have been performed by Varandas and coworkers[73] on DMBE IV. In turn, Pack *et al.*[74,75] used TI methodologies to obtain state-to-state reaction probabilities and collision lifetimes on the DMBE IV PES. This was followed by Kendrick and Pack[76,77] who examined the implications of conical intersections and the geometrical phase on the reaction probability. Leforestier *et al.*[78,79] used a Lanczos formalism based on the Green's function approach to compute cumulative reaction probabilities for $J = 0$ on the DMBE IV PES and helped with the J-shifting approximation to obtain $k(T)$. In turn, TDWP methodologies were employed by Meijer and Goldfield on the DMBE IV PES to calculate reaction probabilities and cross sections for both $J = 0$ and $J > 0$.[80–82]

Sultanov and Balakrishnan performed TI simulations with the ABC code, also employed in the present work, and used both the DMBE IV and TU PESs to determine cumulative reaction probabilities and J-shifting rate constants.[83] In turn, Lin *et al.*[84,85] have reported state-to-state reaction probabilities obtained from TD and TI simulations on the XXZLG and DMBE IV PESs for $J = 0$, while Honvault *et al.*[86] presented differential and integral cross sections for partial waves up to $J = 50$. Additionally, Hankel[87] carried out TD calculations on both the DMBE IV and XXZLG PESs for $J = 0$ and $J > 0$. Moreover, Bargueño *et al.*[88] studied the reaction by means of quantum and statistical approaches using both the DMBE and XXZLG PESs. Integral cross sections have further been obtained by Lin *et al.*[89] with TD methods on the XXZLG PES. Furthermore, Quéméner *et al.*[90] have reported TI quantum scattering calculations of the $H + O_2 \rightarrow OH + O$ reaction using the DIMKP and XXZLG PESs, with the effect of vibrational and rotational excitations on the reactivity being illustrated, and initial and state-to-state reaction probabilities given together with J-shifting thermal rate coefficients and cross sections. Other interesting quantum mechanical studies have recently been reported by Chen and Poirier,[91] and Petty *et al.*,[92] who determined the bound ro-vibrational states of HO_2 up to $J = 130$ on the DMBE IV PES and examined the implications of the J-shifting approximation for the title system.

B. Method

The TI quantum method used in the present work is implemented on the ABC code of Manolopoulos and coworkers,[93] which employs the coupled-channel hyperspherical coordinate formalism to solve the Schrödinger equation of motion for three nuclei on a single Born-Oppenheimer PES. In this approach, the wavefunction of the nuclei is expanded in terms of the hyperspherical arrangement channel basis functions, whose number must be sufficiently large to include all open channels at a given maximum internal energy (E_{max}). Such functions must also account for the total angular momentum quantum number J, the space- and body-fixed projections of J and all asymptotic vibrational and rotational quantum numbers (up to a j_{max} value), and depend on all three Euler angles and the internal Delves hyperspherical angles. The

corresponding coupled-channel equations are integrated using the constant reference potential log-derivative method.[94,95] For each ABC run, the code solves the Schrödinger equation for specified values of the total angular momentum, J, and the triatomic and diatomic parities. From the resulting parity-adapted scattering matrix, for enough energies and values of J, it is possible to determine various dynamical observables such as the differential and total cross sections or even thermal rate coefficients.

As noted in the Introduction, the reactions $O + OH \rightleftharpoons O_2 + H$ present a highly stable intermediate and the energy difference between asymptotes is substantial, with the whole task then implying a huge number of coupled states. Such attributes hinder the performance of computations with large values of the total angular momentum and the entire set of couplings emerging from their projections. To overcome such a computational burden, many approximate methods have been proposed, e.g., the statistical quantum method,[96,97] which has already been employed for the title O + OH reaction.[63,88]

In this work, we have adopted the popular J-shifting scheme,[98] which has been much used in the study of the O + OH direct reaction[60,62,64,65,67–69] and also for the $H + O_2$ reverse channel.[83,90] Since the dynamical problem differs according to the reactive channel, the comparison between the J-shifting rate constants has been distinctly addressed. For O + OH, initial state rate constants are calculated from initial state-selected reaction probabilities, while for the $H + O_2$ reaction we employ initial state and cumulative reaction probabilities (CRP).

Using common notation,[65] the initial state rate constant for the O + OH reaction is calculated as

$$k_{v,j}(T) = \frac{1}{2\pi\hbar Q_R}\left(\sum_J (2J+1)e^{-E^J_{\text{shift}}/(k_B T)}\right) \times \int_0^\infty P^J_{v,j}(E_c)e^{-E_c/(k_B T)}dE_c, \quad (1)$$

where Q_R is the reactants partition function, $Q_R = Q_{trans}Q_{el}$, with the translational partition function being given by

$$Q_{trans} = \left(\frac{\mu k_B T}{2\pi\hbar^2}\right)^{3/2} \quad (2)$$

and the electronic partition function by[47,99]

$$Q_{el} = \frac{(5 + 3e^{-228/T} + e^{-326/T})(2 + 2e^{-205/T})}{2}, \quad (3)$$

where E^J_{shift} denotes the height of the effective barrier for a given partial wave J in the entrance channel, which is obtained by evaluating the effective potential

$$V^J_{eff}(R_{\text{O–OH}}) = \frac{\hbar^2 J(J+1)}{2\mu R^2_{\text{O–OH}}} + V_{min}(R_{\text{O–OH}}). \quad (4)$$

In this equation, $V_{min}(R_{\text{O–OH}})$ is the potential calculated at the equilibrium geometry of the molecule ($r_{eq} = 1.83$ Å) as a function of the atom-molecule center-of-mass distance. The $V_{min}(R_{\text{O–OH}})$ so obtained is in agreement with the values provided in other publications[60,65,67] where the minimum energy path is used.

To determine the $H + O_2$ thermal rate coefficient, the J-shifting approximation is applied to the cumulative reaction probability, with the rate constant given as[90]

$$k(T) = \frac{1}{2\pi\hbar Q_R} Q^\ddagger_{rot} \int_0^\infty N^{J=0}(E)e^{-E/(k_B T)}dE, \quad (5)$$

where $Q_R = Q_{el}Q_{trans}Q_{rot-vib}$ is the partition function per unit of volume of the reactants. Moreover, Q_{trans} has the meaning assigned above, $Q_{el} = 3$, and the ro-vibrational partition function is given by

$$Q_{rot-vib} = \sum_{v,odd\ j} (2j+1)e^{-\epsilon_{O_2}(v,j)/(k_B T)}, \quad (6)$$

where $\epsilon_{O_2}(v, j)$ are the O_2 ro-vibrational energies. In Eq. (6), the summation accounts for all thermally populated levels of O_2. $Q^\ddagger_{rot}$, the partition function of the O···OH complex at the transition state, is evaluated as

$$Q^\ddagger_{rot} = \sum_{J=0}^{\infty}(2J+1)\sum_{K=-J}^{J} e^{-E^\ddagger_{JK}/(k_B T)}. \quad (7)$$

Considering now a symmetric top geometry, one gets for the rotational energy $E^\ddagger_{JK}$ at the transition state

$$E^\ddagger_{JK} = B^\ddagger J(J+1) + (A^\ddagger - B^\ddagger)K^2, \quad (8)$$

where $A^\ddagger$ and $B^\ddagger$ are the rotational constants of the O···OH complex at the transition state. Table I gathers the data here employed which are similar to the ones provided elsewhere,[90] but completed with the transition state geometry and rotational constants determined for the CHIPR PES. Initial state rate coefficients for the $H + O_2$ reaction are calculated using Eq. (5) with $Q_R = Q_{el}Q_{trans}$ and replacing the CRP for the initial state reaction probability.

C. Convergence tests

As stated above, the J-shifting approximation is used to calculate thermal rate coefficients, and hence calculations with total angular momenta $J > 0$ (and corresponding couplings of their projections) need not be explicitly considered. Despite this, the dynamical simulation of this reaction remains highly demanding due to the amount of coupled states required for a proper description.

Since the ABC code sets automatically the number of surface eigenfunctions (coupled states) and its representation basis to limit the computational effort, we can only control the parameters E_{max}, the total energy available in any channel, and j_{max}, the allowed number of rotational states. The convergence of these parameters is then here addressed prior to the convergence of other variables.

TABLE I. Geometry and rotational constants of O···OH complex at the transition state for the DIMKP, XXZLG, DMBE IV and CHIPR PESs.

PES	DIMKP	XXZLG	DMBE IV	CHIPR
R_{OH}/a_0	1.83	1.835	1.82	1.835
R_{OO}/a_0	5.07	5.47	5.08	5.480
$\theta_{OOH}/^o$	34.0	46.9	40.00	46.81
$A^\ddagger/cm^{-1}$	61.28	35.59	44.95	35.51
$B^\ddagger/cm^{-1}$	0.289	0.250	0.289	0.249

As a reference on the number of coupled states, we refer to the work by Sultanov and Balakrishnan[83] who have also used the standard ABC code for thermal rate calculations of the $H + O_2$ reaction using the J-shifting approximation. In their study, the calculated cumulative reaction probability has been obtained by setting $j_{max} = 59$ and $E_{max} = 3.9$ eV (i.e., 933 channels), on the DMBE IV PES,[38] and $j_{max} = 59$ with $E_{max} > 4.2$ eV, while considering 1151 open channels for simulations on the TU PES.[40] To visualize such a high number of states, we address the reader to Figure 3 of the paper by Pack *et al.*,[75] who have plotted the diabatic surface function eigenvalues over a wide range of energies and distances in their study of the $H+O_2$ reaction. Their plot illustrates the number of open $H + O_2$ channels below the $O + OH$ asymptote, and how the strongly bound surface functions are mainly connected diabatically with the $O + OH$ channels rather than the $H + O_2$ ones (the OH bond length and its stretching frequency in the complex are similar to the isolated OH). This implies that a huge number of $O+OH$ channels must be included to correctly describe the title reaction.

Apart from the above reference, not many other works provide details on the study of the title reaction with the ABC code, specially for the $O + OH$ arrangement. Quéméner *et al.*[65,67–69] employed the hyperspherical approach of Pack and Parker[66] in their study of the reaction OH + O $(v = 0,1,2,3; j = 0) \rightarrow O_2 + H$. Although they employ a similar methodology, there are differences in the choice of the basis functions, as reflected on the different numbers of coupled states required for their computations. Specifically, in their study of the $v = 0$ and $v = 1$ initial state rate constant, the authors use $n = 393$ channels and set $\rho_{max} = 26.8$ Å (with larger distances for cold regimes, $\rho_{max} = 44.05$ Å). For $v = 2$ and $v = 3$, values of $n = 619$ and 850 coupled states have been used, respectively.

For the convergence of the $O + OH$ arrangement, special emphasis has been given to the correct determination of the fundamental initial state reaction probability and the corresponding J-shifting thermal rate coefficient. For this reaction, we have obtained convergence with $j_{max} = 50$ and $E_{max} = 3.0$ eV, resulting in over 1400 coupled states. As in precedent studies, special attention has been paid to the energy resolution of the simulations and the convergence of the J-shifting scheme by considering spacings of ~ 0.0002 eV appropriate to correctly resolve the resonance pattern at low kinetic energies. Larger energy spacings (0.001 eV) have been used for higher energies. In turn, the value of ρ_{max} has been set at 27 Å, which lies close to the Quéméner *et al.*[65] one.

For the $H + O_2$ reaction, we have considered for convergence the ABC parameters $E_{max} = 3.6$ eV, $j_{max} = 59$, and $\rho_{max} = 29$ Å, hence a set of values similar to the ones used by Sultanov and Balakrishnan.[83] Note that the value of E_{max} is referred to the corresponding asymptote and so, considering the reaction exothermicity, the provided values are in agreement. However, when comparing the computational cost of each arrangement, one must account for the symmetry of the system, which in this case facilitates the study of the $H + O_2$ reaction. Specifically, only odd numbered rotational states are allowed by symmetry,[100] since ground-state O_2 is a Hund's case (b) molecule.[101] Although the lowest observed rotational state for OH is also known to be the first if the molecule is considered to belong to Hund's case (b),[100] we will also use $j = 0$ as commonly done for the $O + OH$ reaction.

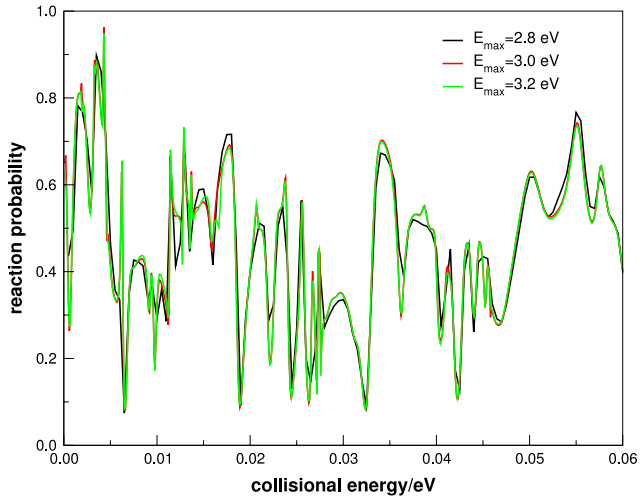

FIG. 1. Convergence tests for E_{max}: initial state reaction probabilities for the reaction $O + OH(v = 0, j = 0) \rightarrow O_2(v = \text{all}, j = \text{all}) + H$ as a function of the collisional energy.

As an example of the E_{max} converging process, we show in Figure 1 the calculated initial state-selected reaction probabilities obtained for the reaction $O + OH(v = 0, j = 0) \rightarrow O_2(v = \text{all}, j = \text{all}) + H$. As shown, the initial state reaction probabilities are nearly coincident with each other for $E_{max} = 3.0$ and 3.2 eV, which led us to consider this parameter as converged with 3.0 eV. It should be noted that despite the fact that results with $E_{max} = 2.8$ eV show only small differences on the calculated resonance pattern (while maintaining the same average value), the corresponding J-shifting rate constants show significant differences, mainly at low temperatures.

III. RESULTS AND DISCUSSION

A. The O + OH arrangement

1. Initial state reaction probabilities

Figure 2 shows initial state reaction probabilities as a function of the collisional energy for the reaction $O + OH$ $(v = 0, j = 0) \rightarrow O_2(v = \text{all}, j = \text{all}) + H$. A comparison between of our results (in black) with other time-independent data available in the literature is also presented. Panels (a) and (b), compare our results with the ones obtained by Quéméner *et al.*[65] on the XXZLG PES (red curve) and the DIMKP PES (green). Despite some difficulty in the data extraction, the main differences on the initial state reaction probabilities are clearly visible. For the energy range shown in Figure 2, the results on the CHIPR, XXZLG, and DIMKP PESs are all in agreement, specially for the average probability, manifesting however a different resonance pattern, since this is more sensitive to subtle differences. As it will be shown later, small differences on the initial state reaction probability, specially at the lower collisional energies, may bear an important impact on the corresponding thermal rate coefficient, so that small variations on the PES can have significant consequences.

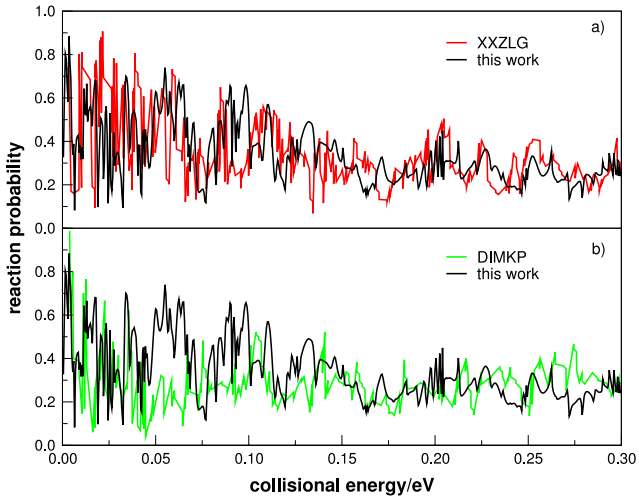

FIG. 2. Reaction probabilities for the O + OH($v = 0, j = 0$) reaction as a function of the collisional energy. Key for panels: (a) comparison with the results from the XXZLG PES; (b) idem, but for DIMKP (data extracted from Quéméner *et al.*[65]).

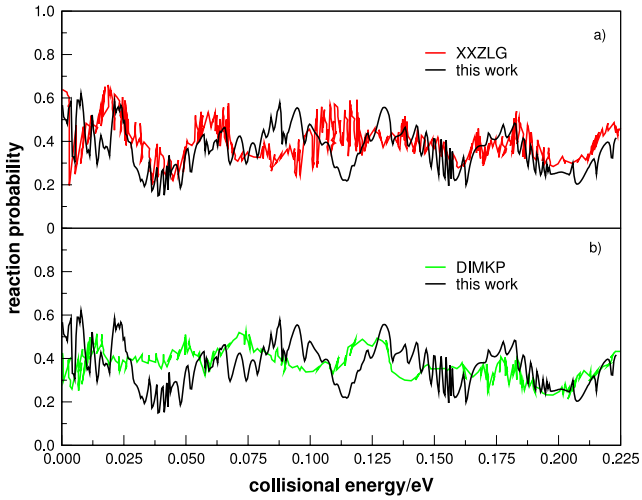

FIG. 4. Reaction probabilities for O + OH($v = 1, j = 0$) as a function of collisional energy. Key for panels: current results vs the ones obtained with XXZLG PES; (b) idem, but for DIMKP PES (data extracted from Juanes-Marcos *et al.*[68]).

For each ABC run, additional important information is obtained. Figure 3 shows initial state reaction probabilities O + OH($v = 0, j$) as a function of the collisional energy. Even (panel (a)) and odd (panel (b)) initial rotational state reaction probabilities are presented separately to simplify the visualization. It is apparent from this plot that the reaction is not enhanced by rotational excitation. Moreover, all reaction probabilities have similar average values, while exhibiting slightly larger probabilities for $j = 0$, but not showing any apparent trend, apart from its characteristic oscillatory pattern that changes when increasing the rotational quantum number. Such results may largely be attributed to the fact that the reaction occurs over deep potential wells, which may contribute to redistribute the internal energy in a more or less statistical way as suggested elsewhere.[63]

To conclude this section, Figure 4 shows reaction probabilities for O + OH($v = 1, j = 0$) → O_2(v = all, j = all) + H as a function of the collisional energy. Also included for comparison are the results extracted from Juanes-Marcos *et al.*[68] as obtained with the XXZLG (panel (a)) and DIMKP (panel (b)) PESs. In their work,[68] the authors highlight the better behavior of the DIMKP PES with respect to the XXZLG results at low collisional energies, where the long-range interactions are dynamically more important. Such differences can be attributed to deficiencies on the long range extrapolated regions of the XXZLG PES. Such features have been corrected in the CHIPR form here utilized.[45] As expected, a better agreement is found between our results and the ones obtained on the XXZLG PES, especially at higher energies, with the average value of the reaction probabilities being essentially the same and, interestingly, presenting the same strong oscillatory pattern but exhibiting differences on the thinner resonance pattern, more sensitive to the long range forces. With respect to the results on the DIMKP PES, the probabilities obtained from the CHIPR and XXZLG PESs present richer and sharper resonance peaks, partly due to their deeper potential wells which support a larger number of states (well depths of 2.246 and 2.326 eV relative to the H + O_2 asymptote, respectively).

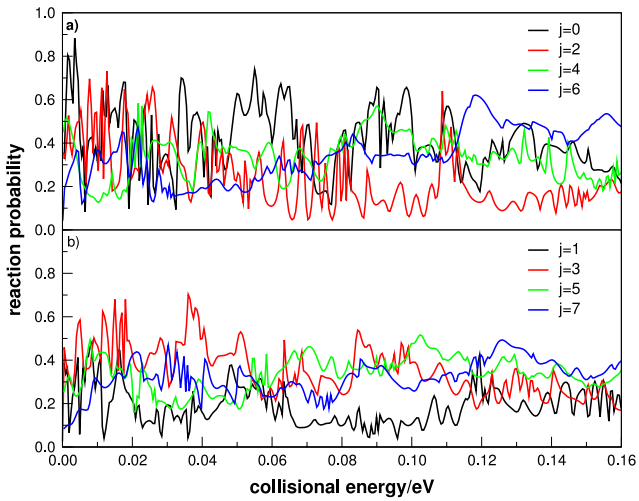

FIG. 3. Reaction probabilities for the O + OH($v = 0, j$) reaction as a function of collisional energy. Key for panels: (a) initial even j values; (b) odd initial j values.

2. Thermal rate coefficients

From the reaction probabilities presented above, J-shifting thermal rate coefficients have been calculated using Eq. (1). Figure 5 shows the calculated results as a function of the temperature jointly with selected experimental data,[6,19,21,22] the theoretical values of Quéméner *et al.*[65] obtained with the XXZLG (red line) and DIMKP (green line) PESs, and the time-independent ones obtained by Lique *et al.*[64] with the XXZLG PES (dashed red). Additionally, the QCT results of Varandas[43] (blue line) have been included since they have also been calculated with the CHIPR PES.

As noted in the Introduction, the experimental data of Carty *et al.*[6] show a different trend from other older experimental results, falling, however, close to the theoretical results. When the latter are compared with each other,

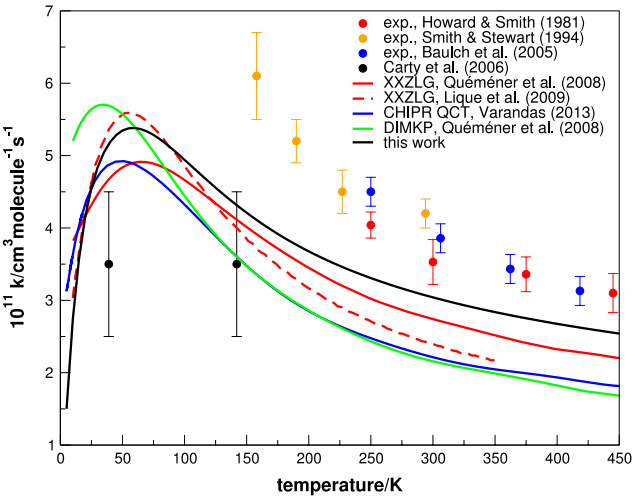

FIG. 5. Rate constants for the reaction O + OH($v = 0, j = 0$) as a function of temperature: from this work (solid black), selected experimental data (black dots,[6] red dots,[19] green dots,[21] and blue dots[22]). Also shown are TI data calculated by Quéméner *al.*[65] (solid red) and Lique *et al.*[64] (red dashed line) on the XXZLG PES, as well as data[65] from DIMKP (green line) and QCT data[43] from CHIPR (blue line).

their similarity is highlighted, showing consistency on the employed methodology and demonstrating that the *J*-shifting scheme can provide acceptable results when judged against the experimental data. Stands out above all the similar trends from our results and the ones provided by Quéméner *et al.*[65] on the XXZLG PES, although ours give somewhat larger thermal rate coefficients over all the temperature range. The different behaviors between the XXZLG PES data, attributed to a different implementation of the *J*-shifting approximation,[65] may reflect how sensitive, and perhaps arbitrary, is the determination of the *J*-shifting rate constant when dealing with such highly structured reaction probabilities. The different behaviors of the DIMKP PES data, with the maximum of the thermal rate coefficient shifted to lower temperatures, providing larger thermal rate coefficients for temperatures below ~100 K, have been explained elsewhere[65] and mostly attributed to the different topologies of the PES, in particular at the region of a small "reef" that arises at the hydrogen-type (in OH···O) to covalent-type bonding transition, which is distinctly located according to the PES. In this regard, we should observe that the attributes of this "reef" in CHIPR[44,45] show close agreement with the most recent, and possibly accurate, *ab initio* calculations[102] for the ground-state PES of the HO_2 system.

From the above, it can be concluded that the *J*-shifting scheme can offer a satisfactory approximation for calculating the rate constant, although a more detailed analysis may be required when the reaction probability is rich in resonances, and hence, small differences on the PES are difficult to translate into the thermal rate coefficient. Calculations accounting for all values of the total angular momentum and its projection are then required, but extremely difficult to perform due to the huge number of involved coupled states. For example, the calculations of Lique *et al.*[64] not only required restrictions on the helicity quantum number but also over 9000 channels employing an energy grid ranging from 2.4×10^{-4} to 0.038 eV, while using the *J*-shifting approximation above this energy. In fact, the rate constant so obtained turns out to be at least 20%-30% larger than its *J*-shifting value. Such calculations are beyond the scope of the present work.

Regarding the QCT results of Varandas[43] on CHIPR, they show a pattern similar to the quantum theoretical results but provide somewhat smaller thermal rate coefficients. This may attributed to the fact that the QCT method does not include quantum effects and that the reactivity is highly determined by the influence of the intermediate complex and the metastable states formed during the reactive encounter.

Reactive rate constants obtained by applying the *J*-shifting approximation to O + OH($v = 1, j = 0$) collisions are presented in Figure 6, jointly with available theoretical and experimental data. All our results, in black, have been obtained by setting the maximum energy parameter to $E_{max} = 3.2$ eV. Note that the points represent the collisional removal data of OH($v = 1$) by O atoms, the thermal rate coefficient of Khachatrian and Dagdigian,[103] and the QCT results of Varandas[51] on the DMBE IV PES (black points). Note further that the time-independent results have been extracted from Juanes-Marcos *et al.*,[68] where both the XXZLG and DIMKP PESs have been used. As commented by the authors, the reported rate constant for collisional removal at room temperature is about $(3.9\pm0.6)\times10^{-11}$ cm^3 molecule^{-1} s^{-1} but, since this total removal rate coefficient contains contributions from both chemical reaction and vibrational relaxation whose branching ratios are estimated to be 85% and 15%, the final reported value for the rate constant with OH($v = 1$) is $(3.3\pm0.5)\times10^{-11}$ cm^3 molecule^{-1} s^{-1}, thence in good agreement with the quantum theoretical predictions and the QCT results of Varandas at $T = 255$ K. Regarding high temperatures, the reported thermal rate coefficients are in satisfactory agreement with the results obtained from other PESs. Conversely, the behavior at low temperatures is different, with our results lying between the other theoretical data. With the results on the XXZLG PES showing overall a higher absolute value, and the

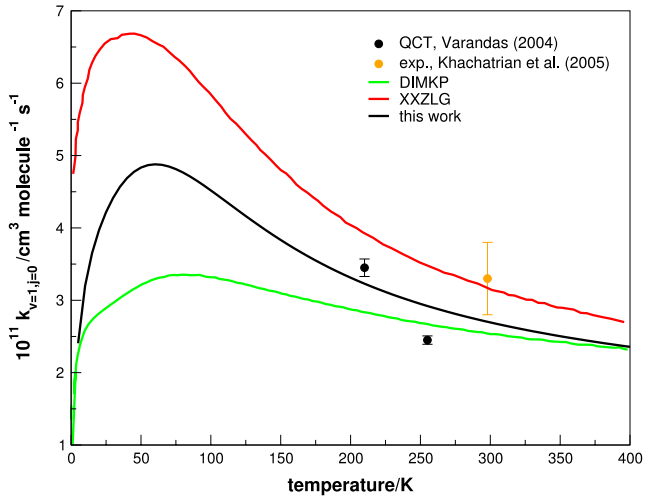

FIG. 6. Initial state-selected rate constants for the O + OH($v = 1, j = 0$) reaction as a function of temperature. Key for lines: from this work (black) on the XXZLG PES (red); from DIMKP PES (green). Also shown are experimental data of Khachatrian and Dagdigian[103] (blue dot) and QCT results of Varandas[51] on the DMBE IV PES (black dots).

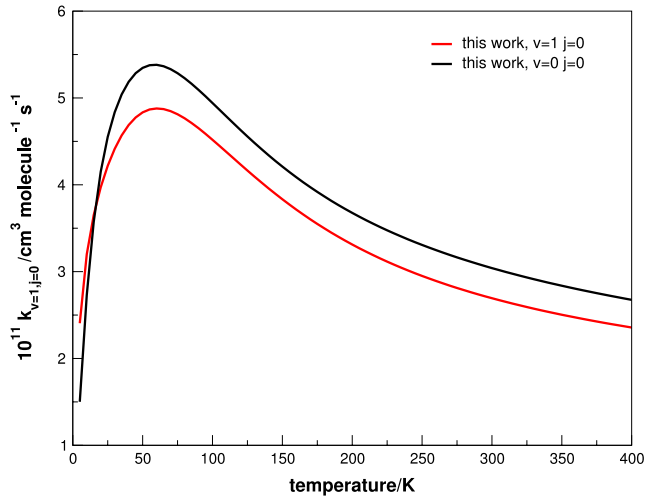

FIG. 7. J-shifting rate constants for specific initial vibrational states.

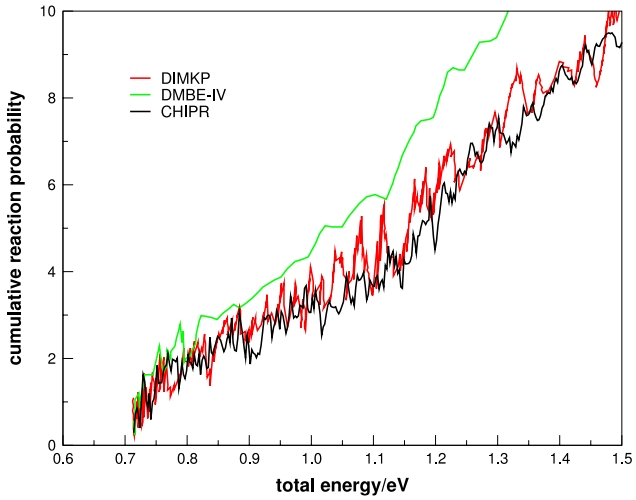

FIG. 8. Cumulative reaction probabilities for the H+O_2 reaction as a function of the energy. Key for lines: this work from CHIPR (in black), and the previously reported data by Sultanov and Balakrishnan from DMBE[83] (green) and DIMKP[90] (red).

DIMKP ones being somewhat lower, they display though a similar profile.

On studying the effect of vibrational excitation on the reactivity, Figure 7 suggests that increasing the vibrational state of OH may lead to thermal rate coefficients roughly of the same magnitude and a similar temperature dependence but with a decreasing reactivity with the vibrational state of OH. Differently, the reported thermal rate coefficients on the XXZLG PES[68] increase when going from $v = 0$ to $v = 1$. Moreover, according to the results[68,69] on the DIMKP PES, there is a drop of the reactivity presenting a different temperature dependence. In their latest article,[69] the authors also provide data for initial vibrational states $v = 2$ and $v = 3$, which behave similarly to v=1 by showing an increase in reactivity when increasing the vibrational state. The authors attribute the special behavior of the $v = 0$ thermal rate coefficient, which crosses other the $v = 1$ curve, to the presence of quasi-bound states near the O+OH($v = 0, j = 0$) dissociation threshold that enhances the reaction.[68] Showing a somewhat distinct behavior as a function of the temperature according the PES employed, our results for the thermal rate coefficient are consistent with the assumption made in atmospheric kinetic models[23,104] that predict a relatively small dependence on the initial vibrational quantum number for the O + OH reaction.

B. The H + O_2 arrangement

Figure 8 shows the calculated CRP for the H + O_2 reaction as a function of the total energy. Regarding the current CRP results (black), they have been obtained from simulations with the converged parameters reported above, mainly using E_{max} = 3.6 eV, $j_{max} = 59$, $\rho_{max} = 29$ a_0, thus values similar to the ones employed by Sultanov and Balakrishnan[83] in their TI study with DMBE IV. Also included in this figure are data extracted from Quéméner *et al.*,[90] which were obtained from calculations with the DMBE IV (green) and DIMKP (red) PESs. To perform this comparison, the probabilities have been shifted to the same energy since the various PESs show different energy thresholds. The XXZLG data, also available in their work,[90] have not been included since it is roughly similar to the DIMKP result (difficult to extract) and not required for the present discussion. The most prominent result from Figure 8 is perhaps the similar trend shown by the results obtained from the CHIPR and DIMKP (and XXZLG) PESs, and the somewhat larger differences with the results obtained from the DMBE IV PES, already discussed in the literature[80,84,87,90] and attributed to an onset of a direct reaction mechanism. When comparing such data, and obviating the DMBE results, the global picture is similar, with small differences only observed in the resonance pattern of the initial state and cumulative reaction probabilities. However, important differences arise when translating this information to the determination of the thermal rate coefficient.

Figure 9 shows the Arrhenius plot of the thermal rate coefficient as a function of $1000/T$ together with other published theoretical and experimental data. All theoretical results

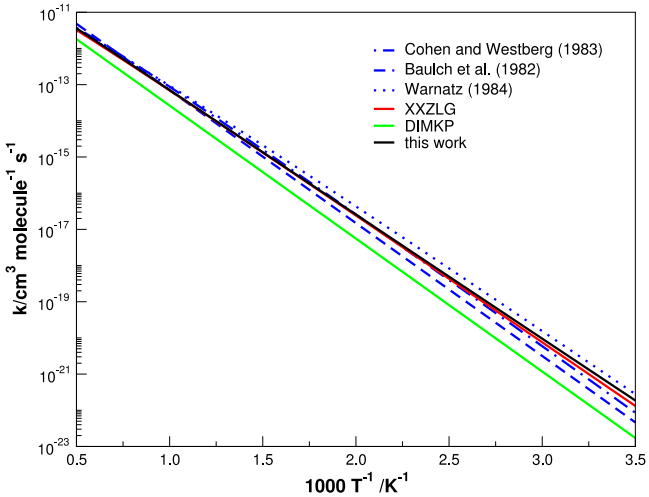

FIG. 9. Thermal rate coefficients for the H + O_2 reaction. Key for lines: from this work (in black); using the DIMKP (red), and XXZLG (green) PESs.[90] Also shown are the fitted experimental results of Baulch,[36] Cohen and Westberg,[30] and Warnatz.[105]

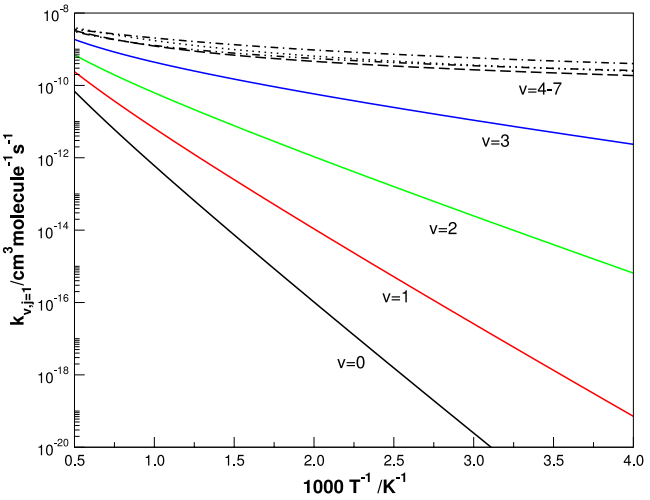

FIG. 10. Initial state rate constants for the H + $O_2(v = 0 - 7, j = 1)$ reaction: enhancement of reactivity with increasing vibrational state of the O_2 molecule.

have been obtained with the J-shifting approximation and, as observed in the previous paragraph, important differences appear when comparing the DIMKP results with the ones calculated from the CHIPR and XXZLG PESs. As stated by Quéméner,[90] for this reaction, the relative weight of the $Q^{\ddagger}_{rot}$ in the rate constant is crucial and so is obviously the geometry of the transition state and rotational constant associated with each PES. Since the TS configurations of the XXZLG and CHIPR PESs are essentially the same, the resulting thermal rate coefficients are similar, unlike the DIMKP results, despite having a similar CRP. Regarding the comparison between the results from the CHIPR PES and the experimental data, no significant differences are observed, particularly at low and intermediate temperatures. In fact, the calculated results seem to support here too the use of the J-shifting approximation for the study of the $H + O_2$ reaction.

In contrast with the other reactive channel, the vibrational excitation of the reactants is shown to considerably enhance reactivity for the title arrangement. To observe this effect, Figure 10 shows vibrational initial state-selected rate constants for the $H + O_2(v, j = 1)$ reaction, with initial vibrational rate constants up to $v = 7$ being considered. One observes that reactivity is enhanced when increasing the initial vibrational state of O_2 up to $v = 4$. From this vibrational state onwards, the contribution to reactivity is about the same, since one has reached an initial internal energy above the reaction endothermicity. This study of the reactivity is analogous to the presented by Quéméner *et al.*,[90] where the authors compare the same observable but obtained from calculations with the DIMKP and XXZLG PESs.

IV. CONCLUSIONS

We have reported TI calculations of thermal rate coefficients for the reactions $O + OH \rightleftharpoons O_2 + H$ on the recently reported CHIPR PES, which are calibrated from the same *ab initio* data as the XXZLG one but provides a refinement of the latter particularly at the long range interaction regions. This should be key for the O + OH reaction when studying reactivity under low- and very-low temperature regimes. All calculations have employed the popular J-shifting approximation. The reported initial state reaction probabilities for the O + OH $(v = 0, j = 0)$ show features analogous to the ones determined from the XXZLG PES, although exhibiting differences at low collisional energies where the different long range descriptions are noticeable. Similarly, the calculated rate constants are predicted in fair agreement with previously reported TI ones, except for small differences both at low- and (in absolute value) high-temperature regimes. In fact, the results indicate that the J-shifting approximation performs well for the title system but suggests that the method may not be optimal for a comparative analysis of PESs. Additionally, the initial state thermal rate coefficients for the $O + OH(v = 1, j = 0)$ reaction exhibit a similar behavior as for $v = 0$, in agreement with current chemical models. Regarding the calculated $H + O_2$ thermal rate coefficients, they are predicted in good agreement with previous calculations, which is mostly due to being controlled by the reaction endothermicity. Most proeminently from the results of the present work is, perhaps, the fact that CHIPR is likely to be the most accurate global PES so far reported for HO_2, thence being commended for further dynamics studies.

ACKNOWLEDGMENTS

This work has the support of Fundação para a Ciência e a Tecnologia, Portugal, under contracts PTDC/CEQ-COM3249/2012 and PTDC/AAG-MAA/4657/2012, as well as the support to the Coimbra Chemistry Centre through the project PEst-OE/QUI/UI0313/2014.

[1]I. W. M. Smith, E. Herbst, and Q. Chang, Mon. Not. R. Astron. Soc. **350**, 323 (2004).
[2]R. Wayne, *Chemistry of Atmospheres* (Oxford University Press, 2000).
[3]U. Hincelin, V. Wakelam, F. Hersant, S. Guilloteau, J. C. Loison, P. Honvault, and J. Troe, Astron. Astrophys. **530**, A61 (2011).
[4]L. Reboussin, V. Wakelam, S. Guilloteau, and F. Hersant, Mon. Not. R. Astron. Soc. **440**, 3557 (2014).
[5]E. Herbst and W. Klempere, Astrophys. J. **185**, 505 (1973).
[6]D. Carty, A. Goddard, S. Kohler, I. Sims, and I. Smith, J. Phys. Chem. A **110**, 3101 (2006).
[7]D. Quan, E. Herbst, T. J. Millar, G. E. Hassel, S. Lin, H. Guo, P. Honvault, and D. Xie, Astrophys. J. **681**, 1318 (2008).
[8]D. Hollenbach, M. J. Kaufman, E. A. Bergin, and G. J. Melnick, Astrophys. J. **690**, 1497 (2009).
[9]E. B. Jenkins, Astrophys. J. **700**, 1299 (2009).
[10]M. Agúndez and V. Wakelam, Chem. Rev. **113**, 8710 (2013).
[11]P. F. Goldsmith, R. Liseau, T. A. Bell, J. H. Black, J.-H. Chen, D. Hollenbach, M. J. Kaufman, D. Li, D. C. Lis, G. Melnick, D. Neufeld, L. Pagani, R. Snell, A. O. Benz, E. Bergin, S. Bruderer, P. Caselli, E. Caux, P. Encrenaz, E. Falgarone, M. Gerin, J. R. Goicoechea, A. Hjalmarson, B. Larsson, J. L. Bourlot, F. L. Petit, M. D. Luca, Z. Nagy, E. Roueff, A. Sandqvist, F. van der Tak, E. F. van Dishoeck, C. Vastel, S. Viti, and U. Yildiz, Astrophys. J. **737**, 96 (2011).
[12]G. J. Melnick, V. Tolls, P. F. Goldsmith, M. J. Kaufman, D. J. Hollenbach, J. H. Black, P. Encrenaz, E. Falgarone, M. Gerin, A. Hjalmarson, D. Li, D. C. Lis, R. Liseau, D. A. Neufeld, L. Pagani, R. L. Snell, F. van der Tak, and E. F. van Dishoeck, Astrophys. J. **752**, 26 (2012).
[13]R. Liseau, P. F. Goldsmith, B. Larsson, L. Pagani, P. Bergman, J. Le Bourlot, T. A. Bell, A. O. Benz, E. A. Bergin, P. Bjerkeli, J. H. Black, S. Bruderer, P. Caselli, E. Caux, J.-H. Chen, M. de Luca, P. Encrenaz, E. Falgarone, M. Gerin, J. R. Goicoechea, Å. Hjalmarson, D. J. Hollenbach, K. Justtanont, M. J. Kaufman, F. Le Petit, D. Li, D. C. Lis, G. J. Melnick, Z. Nagy, A. O. H. Olofsson, G. Olofsson, E. Roueff, Aa. Sandqvist, R. L. Snell, F. F. S. van der Tak, E. F. van Dishoeck, C. Vastel, S. Viti, and U. A. Yildiz, Astron. Astrophys. **541**, A73 (2012).

[14]U. A. Yildiz, K. Acharyya, P. Goldsmith, E. F. van Dishoeck, G. Melnick, R. Snell, R. Liseau, J.-H. Chen, L. Pagani, E. Bergin, P. Caselli, E. Herbst, L. Kristensen, R. Visser, D. Lis, and M. Gerin, Astron. Astrophys. **558**, A58 (2013).
[15]L. Pagani, A. O. H. Olofsson, P. Bergman, P. Bernath, J. H. Black, R. S. Booth, V. Buat, J. Crovisier, C. L. Curry, P. J. Encrenaz, E. Falgarone, P. A. Feldman, M. Fich, H. G. Floren, U. Frisk, M. Gerin, E. M. Gregersen, J. Harju, T. Hasegawa, Å. Hjalmarson, L. E. B. Johansson, S. Kwok, B. Larsson, A. Lecacheux, T. Liljeström, M. Lindqvist, R. Liseau, K. Mattila, G. F. Mitchell, L. H. Nordh, M. Olberg, G. Olofsson, I. Ristorcelli, Aa. Sandqvist, F. von Scheele, G. Serra, N. F. Tothill, K. Volk, T. Wiklind, and C. D. Wilson, Astron. Astrophys. **402**, L77 (2003).
[16]B. Larsson, R. Liseau, L. Pagani, P. Bergman, P. Bernath, N. Biver, J. Black, R. S. Booth, V. Buat, J. Crovisier, C. L. Curry, M. Dahlgren, P. Encrenaz, E. Falgarone, P. Feldman, M. Fich, H. Floren, M. Fredrixon, U. Frisk, G. Gahm, M. Gerin, M. Hagstrom, J. Harju, T. Hasegawa, A. Hjalmarson, L. Johansson, K. Justtanont, A. Klotz, E. Kyrola, S. Kwok, A. Lecacheux, T. Liljestrom, E. Llewellyn, S. Lundin, G. Megie, G. Mitchell, D. Murtagh, L. Nordh, L.-A. Nyman, M. Olberg, A. Olofsson, G. Olofsson, H. Olofsson, G. Persson, R. Plume, H. Rickman, I. Ristorcelli, G. Rydbeck, A. Sandqvist, F. Scheele, G. Serra, S. Torchinsky, N. Tothill, K. Volk, T. Wiklind, C. Wilson, A. Winnberg, and G. Witt, Astron. Astrophys. **466**, 999 (2007).
[17]M. Howard and I. Smith, Chem. Phys. Lett. **69**, 40 (1980).
[18]R. S. Lewis and R. T. Watson, J. Phys. Chem. **84**, 3495 (1980).
[19]M. J. Howard and I. W. M. Smith, J. Chem. Soc., Faraday Trans. 2 **77**, 997 (1981).
[20]W. H. Brune, J. J. Schwab, and J. G. Anderson, J. Phys. Chem. **87**, 4503 (1983).
[21]I. W. M. Smith and D. W. A. Stewart, J. Chem. Soc., Faraday Trans. **90**, 3221 (1994).
[22]D. L. Baulch, C. Bowman, C. Cobos, R. Cox, T. Just, J. Kerr, M. Pilling, D. Stocker, J. Troe, W. Tsang, R. Walker, and J. J. Warnatz, J. Phys. Chem. Ref. Data **34**, 757 (2005).
[23]R. Robertson and G. P. Smith, J. Phys. Chem. A **110**, 6673 (2006).
[24]V. Wakelam, E. Herbst, J.-C. Loison, I. W. M. Smith, V. Chandrasekaran, B. Pavone, N. G. Adams, M.-C. Bacchus-Montabonel, A. Bergeat, K. Béroff, V. M. Bierbaum, M. Chabot, A. Dalgarno, E. F. van Dishoeck, A. Faure, W. D. Geppert, D. Gerlich, D. Galli, E. Hébrard, F. Hersant, K. M. Hickson, P. Honvault, S. J. Klippenstein, S. L. Picard, G. Nyman, P. Pernot, S. Schlemmer, F. Selsis, I. R. Sims, D. Talbi, J. Tennyson, J. Troe, R. Wester, and L. Wiesenfeld, Astrophys. J., Suppl. Ser. **199**, 21 (2012).
[25]J. Woodall, M. Agúndez, A. J. Markwick-Kemper, and T. J. Millar, Astron. Astrophys. **466**, 1197 (2007).
[26]R. Atkinson, D. L. Baulch, R. Cox, J. Crowley, R. Hampson, R. G. Hynes, M. Jenkin, M. Rossi, and J. Troe, Atmos. Chem. Phys. **4**, 1461 (2004).
[27]S. P. Sander, J. Abbatt, J. R. Barker, J. B. Burkholder, R. R. Friedl, D. M. Golden, R. E. Huie, C. E. Kolb, M. J. Kurylo, G. Moortgat, V. L. Orkin, and P. H. Wine, *Chemical Kinetics and Photochemical Data for Use in Atmospheric Studies Evaluation Number 17* (JPL Publication 10-6, Jet Propulsion Laboratory, Pasadena, 2011).
[28]G. L. Schott, Combust. Flame **21**, 357 (1973).
[29]D. L. Baulch, R. A. Cox, P. J. Crutzen, R. F. Hampson, J. A. Kerr, J. Troe, and R. T. Watson, J. Phys. Chem. Ref. Data **11**, 327 (1982).
[30]N. Cohen and K. R. Westberg, J. Phys. Chem. Ref. Data **12**, 531 (1983).
[31]N. Fujii and K. S. Shin, Chem. Phys. Lett. **151**, 461 (1988).
[32]A. N. Pirraglia, J. V. Michael, J. W. Sutherland, and R. B. Klemm, J. Phys. Chem. **93**, 282 (1989).
[33]D. A. Masten, R. K. Hanson, and C. T. Bowman, J. Phys. Chem. **94**, 7119 (1990).
[34]T. Yuan, C. Wang, C. L. Yu, M. Frenklach, and M. J. Rabinowitz, J. Phys. Chem. **95**, 1258 (1991).
[35]K. S. Shin and J. V. Michael, J. Chem. Phys. **95**, 262 (1991).
[36]D. L. Baulch, C. J. Cobos, R. A. Cox, P. Frank, G. Hayman, T. Just, J. A. Kerr, T. Murrells, M. J. Pilling, J. Troe, R. W. Walker, and J. Warnatz, J. Phys. Chem. Ref. Data **23**, 847 (1994).
[37]C. Melius and R. Blint, Chem. Phys. Lett. **64**, 183 (1979).
[38]M. R. Pastrana, L. A. M. Quintales, J. Brandão, and A. J. C. Varandas, J. Phys. Chem. **94**, 8073 (1990).
[39]B. Kendrick and R. T Pack, J. Chem. Phys. **102**, 1994 (1995).
[40]J. Troe and V. G. Ushakov, J. Chem. Phys. **115**, 3621 (2001).
[41]C. Xu, D. Xie, D. H. Zhang, S. Y. Lin, and H. Guo, J. Chem. Phys. **122**, 244305 (2005).
[42]D. Xie, C. Xu, T.-S. Ho, H. Rabitz, G. Lendvay, S. Y. Lin, and H. Guo, J. Chem. Phys. **126**, 074315 (2007).
[43]A. J. C. Varandas, J. Chem. Phys. **138**, 134117 (2013).
[44]A. J. C. Varandas, "Putting together the pieces: Global description of valence and long-range forces via combined hyperbolic inverse-power representation of the potential energy surface for use in reaction dynamics," in *Reaction Rate Constant Computations: Theories and Applications* (The Royal Society of Chemistry, UK, 2014), pp. 408–445.
[45]A. J. C. Varandas, J. Chem. Phys. **138**, 054120 (2013).
[46]P. F. Weck and N. Balakrishnan, Int. Rev. Phys. Chem. **25**, 283 (2006).
[47]A. J. C. Varandas, Faraday Discuss. Chem. Soc. **84**, 351 (1987).
[48]J. M. C. Marques and A. J. C. Varandas, Phys. Chem. Chem. Phys. **3**, 505 (2001).
[49]L. A. M. Quintales, A. J. C. Varandas, and J. M. Alvariño, J. Phys. Chem. **92**, 4552 (1988).
[50]A. J. C. Varandas and J. M. C. Marques, J. Chem. Phys. **97**, 4050 (1992).
[51]A. J. C. Varandas, Chem. Phys. Lett. **396**, 182 (2004).
[52]A. J. C. Varandas, Chem. Phys. Lett. **439**, 386 (2007).
[53]M. Jorfi, P. Honvault, P. Halvick, S. Lin, and H. Guo, Chem. Phys. Lett. **462**, 53 (2008).
[54]C. M. Rio, W. Wang, and J. Brandão, J. Mol. Struct.: THEOCHEM **946**, 2 (2010).
[55]T. Stoecklin, B. Bussery-Honvault, P. Honvault, and F. Dayou, Comput. Theor. Chem. **990**, 39 (2012).
[56]A. J. C. Varandas, Mol. Phys. **85**, 1159 (1995).
[57]A. J. C. Varandas, Chem. Phys. Lett. **235**, 111 (1995).
[58]D. E. Skinner, T. C. Germann, and W. H. Miller, J. Phys. Chem. A **102**, 3828 (1998).
[59]T. C. Germann and W. H. Miller, J. Phys. Chem. A **101**, 6358 (1997).
[60]C. Xu, D. Xie, P. Honvault, S. Y. Lin, and H. Guo, J. Chem. Phys. **127**, 024304 (2007).
[61]P. Honvault and J.-M. Launay, in *Theory of Chemical Reaction Dynamics*, edited by A. Laganà and G. Lendvay (Kluwer, Dordrecht, 2004), p. 187.
[62]S. Y. Lin, H. Guo, P. Honvault, C. Xu, and D. Xie, J. Chem. Phys. **128**, 014303 (2008).
[63]M. Jorfi, P. Honvault, P. Bargueño, T. González-Lezana, P. Larrégaray, L. Bonnet, and P. Halvick, J. Chem. Phys. **130**, 184301 (2009).
[64]F. Lique, M. Jorfi, P. Honvault, P. Halvick, S. Y. Lin, H. Guo, D. Q. Xie, P. J. Dagdigian, J. Kłos, and M. H. Alexander, J. Chem. Phys. **131**, 221104 (2009).
[65]G. Quéméner, N. Balakrishnan, and B. K. Kendrick, J. Chem. Phys. **129**, 224309 (2008).
[66]R. T Pack and G. A. Parker, J. Chem. Phys. **87**, 3888 (1987).
[67]G. Quéméner, N. Balakrishnan, and B. K. Kendrick, Phys. Rev. A **79**, 022703 (2009).
[68]J. C. Juanes-Marcos, G. Quéméner, B. K. Kendrick, and N. Balakrishnan, Phys. Chem. Chem. Phys. **13**, 19067 (2011).
[69]G. B. Pradhan, J. C. Juanes-Marcos, N. Balakrishnan, and B. K. Kendrick, J. Chem. Phys. **139**, 194305 (2013).
[70]J. Ma, S. Y. Lin, H. Guo, Z. Sun, D. H. Zhang, and D. Xie, J. Chem. Phys. **133**, 054302 (2010).
[71]J. A. Kłos, F. Lique, M. H. Alexander, and P. J. Dagdigian, J. Chem. Phys. **129**, 064306 (2008).
[72]J. A. Miller, J. Chem. Phys. **74**, 5120 (1981).
[73]A. J. C. Varandas, J. Brandão, and M. R. Pastrana, J. Chem. Phys. **96**, 5137 (1992).
[74]R. T Pack, E. A. Butcher, and G. A. Parker, J. Chem. Phys. **99**, 9310 (1993).
[75]R. T Pack, E. A. Butcher, and G. A. Parker, J. Chem. Phys. **102**, 5998 (1995).
[76]B. Kendrick and R. T Pack, J. Chem. Phys. **104**, 7475 (1996).
[77]B. Kendrick and R. T Pack, J. Chem. Phys. **104**, 7502 (1996).
[78]C. Leforestier and W. H. Miller, J. Chem. Phys. **100**, 733 (1994).
[79]A. Viel, C. Leforestier, and W. H. Miller, J. Chem. Phys. **108**, 3489 (1998).
[80]A. J. H. M. Meijer and E. M. Goldfield, J. Chem. Phys. **108**, 5404 (1998).
[81]A. J. H. M. Meijer and E. M. Goldfield, J. Chem. Phys. **110**, 870 (1999).
[82]E. M. Goldfield and A. J. H. M. Meijer, J. Chem. Phys. **113**, 11055 (2000).
[83]R. A. Sultanov and N. Balakrishnan, J. Phys. Chem. A **108**, 8759 (2004).
[84]S. Y. Lin, H. Guo, P. Honvault, and D. Xie, J. Phys. Chem. B **110**, 23641 (2006).
[85]S. Y. Lin, E. J. Rackham, and H. Guo, J. Phys. Chem. A **110**, 1534 (2006).
[86]P. Honvault, S. Y. Lin, D. Xie, and H. Guo, J. Phys. Chem. A **111**, 5349 (2007).
[87]M. Hankel, S. C. Smith, and A. J. H. M. Meijer, J. Chem. Phys. **127**, 064316 (2007).
[88]P. Bargueño, T. González-Lezana, P. Larrégaray, L. Bonnet, J.-C. Rayez, M. Hankel, S. C. Smith, and A. J. H. M. Meijer, J. Chem. Phys. **128**, 244308 (2008).

[89]S. Y. Lin, Z. Sun, H. Guo, D. H. Zhang, P. Honvault, D. Xie, and S.-Y. Lee, J. Phys. Chem. A **112**, 602 (2008).
[90]G. Quéméner, B. K. Kendrick, and N. Balakrishnan, J. Chem. Phys. **132**, 014302 (2010).
[91]W. Chen and B. Poirier, J. Theor. Comput. Chem. **09**, 435 (2010).
[92]C. Petty, W. Chen, and B. Poirier, J. Phys. Chem. A **117**, 7280 (2013).
[93]D. Skouteris, J. Castillo, and D. Manolopoulos, Comput. Phys. Commun. **133**, 128 (2000).
[94]B. Johnson, J. Comput. Phys. **13**, 445 (1973).
[95]D. E. Manolopoulos, J. Chem. Phys. **85**, 6425 (1986).
[96]E. J. Rackham, F. Huarte-Larranaga, and D. E. Manolopoulos, Chem. Phys. Lett. **343**, 356 (2001).
[97]E. J. Rackham, T. González-Lezana, and D. E. Manolopoulos, J. Chem. Phys. **119**, 12895 (2003).
[98]J. M. Bowman, J. Phys. Chem. **95**, 4960 (1991).
[99]M. M. Graff and A. F. Wagner, J. Chem. Phys. **92**, 2423 (1990).
[100]A. J. C. Varandas, J. Chem. Phys. **99**, 1076 (1993).
[101]G. Herzberg, *Molecular Spectra and Molecular Structure. I. Spectra of Diatomic Molecules*, 2nd ed. (Van Nostrand, New York, 1950).
[102]A. J. C. Varandas, J. Phys. Chem. A **117**, 7393 (2013).
[103]A. Khachatrian and P. J. Dagdigian, Chem. Phys. Lett. **415**, 1 (2005).
[104]R. Robertson and G. P. Smith, Chem. Phys. Lett. **358**, 157 (2002).
[105]J. Warnatz, in *Combustion Chemistry*, edited by W. C. Gardiner (Springer-Verlag, New York, 1984).